



24 amplification was completed, the PCR products were quantified using the Qubit HS dsDNA kit  
25 (ThermoFisher Scientific) and with the Agilent DNA 12000 Bioanalyzer protocol to quantify  
26 amplicon length based on the GenDX NGSgo-AmpX kit estimates. (For HLA-A, -B and -C PCR  
27 products, sizes were 3 kbp to 4 kbp; DRB1 and DRB3 sizes were 3.7 kbp to 4 kbp; DRB4 and  
28 DPB1 contained two expected PCR products, the DRB4 products at 400 bp and 1.5 kb, and the  
29 DPB1 products at 5.0 kbp and 5.7 kbp; DRB5 products were 4 kbp; DQA1 products were 5.5 kbp  
30 to 5.8 kbp; DQB1 amplicons were quantified to be 3.7 kbp to 4kbp; DPA1 amplicons were 4.7 kbp  
31 in length) The amplified PCR products were purified using a bead wash condition of 0.6X volume  
32 of AMPure PB Beads (Pacific Biosciences, part no. 100-265-900) and further eluted in 30  $\mu$ l of  
33 elution buffer (Zymo Research).

#### 34 **Single molecule real-time library preparation, DNA sequencing, and HLA typing**

35 Purified PCR products were normalized to equal concentrations and all amplicons were pooled  
36 per sample and quantified using the Qubit HS dsDNA protocol (ThermoFisher) and the Agilent  
37 DNA 12000 Bioanalyzer protocol. 500 ng of pooled product from each sample was then brought  
38 through the PacBio Amplicon Template Preparation and Sequencing protocol for SMRTbell library  
39 preparation, using the SMRTbell template Prep Kit 1.0 (part no. 100-222-300) using the 0.6X  
40 AMPure PB bead size selection condition. SMRTbell libraries for DRB4 amplicons were prepped  
41 separately in order to adequately sequence the 400 bp exon 2, using a 1.0X Ampure PB bead  
42 size selection followed by each library barcoded individually using SMRTbell Barcoded Adapters  
43 (part no. 100-465-900) and multiplexed.

44 The recommended 20:1 primer:template ratio was used for primer annealing, whereas P6  
45 polymerase binding was performed at a modified 3:1 polymerase to template ratio for DRB4  
46 amplicon SMRTbells and a 10:1 ratio for all other SMRTbells. HLA SMRTbell libraries were  
47 immobilized onto SMRT cells at a concentration of 150 pM on-chip for DRB4 amplicons and 70  
48 pM on-chip for all other products. Loading titrations were performed to achieve optimal

49 sequencing conditions when specific samples required perturbation to achieve optimal loading  
50 parameters. SMRT sequencing was then performed on the RSII system. Long Amplicon Analysis  
51 pipeline v2 (LAA2) was used to process reads and generate .FASTQ files which were imported  
52 into the NGSengine v2.7.0 (GenDX) software for haplotyping and allele annotation, SNP  
53 identification, and individual base calling prior to additional analyses.

#### 54 **Neoantigen prediction pipeline**

55 The novel composite score for neoantigen prediction incorporated the predicted MHC binding  
56 affinity (IC50) to cognate HLA, position of the mutation in the short predicted peptide (with or  
57 without major anchor motif), Levenshtein distance from the nearest self-epitope, expression in the  
58 The Cancer Genome Atlas (TCGA) UC cohort (measured as reads per kilobase of transcript per  
59 million reads mapped [RPKM]), [1] variant allelic frequency (VAF), and prior wildtype (WT) protein  
60 immunogenicity for IgG reactivity using a database of seromic protein microarray reactivity of sera  
61 from multiple cancer types (10,380 protein transcripts, Invitrogen/ThermoFisher's ProtoArrays).  
62 The greatest weight was applied to the IC50, scored as a percentile out of a maximum of 500 nM.  
63 For point mutations located in a canonical binding position (second or last position for most HLA  
64 types), the IC50 of the WT peptide was subtracted from the scoring. Distance from nearest self  
65 was normalized by peptide length, favoring epitopes with unique features. TCGA expression and  
66 potential for seroreactivity were incorporated as score enhancers if detected.

67 Each peptide contained up to 25 amino acids to encompass either a point mutation at its  
68 center or a new frameshift sequence to allow for natural epitope processing and HLA class II  
69 presentation. Up to 20 long polypeptides were synthesized per patient (online supplemental tables  
70 S2-S8), with the majority achieving >85% purity (Genscript, Biosynthesis).

71 The formula for peptide scoring was as follows (subtraction of WT IC50 was only  
72 performed for mutations in an anchor position, not for those in a middle position):

73  $(5000 - (\text{variant IC50} - \text{WT IC50}) / 5000) \times (\text{peptide length} / (\text{peptide length} - \text{distance from}$   
74  $\text{nearest self} - 0.3 \times \lfloor (9 - \text{peptide length}) \rfloor) \times (\text{frequency of seromic detections} / 10 + 1) \times ((\log(\text{TCGA}$   
75  $\text{RPKM}) + 10) / 10) * \text{VAF}$

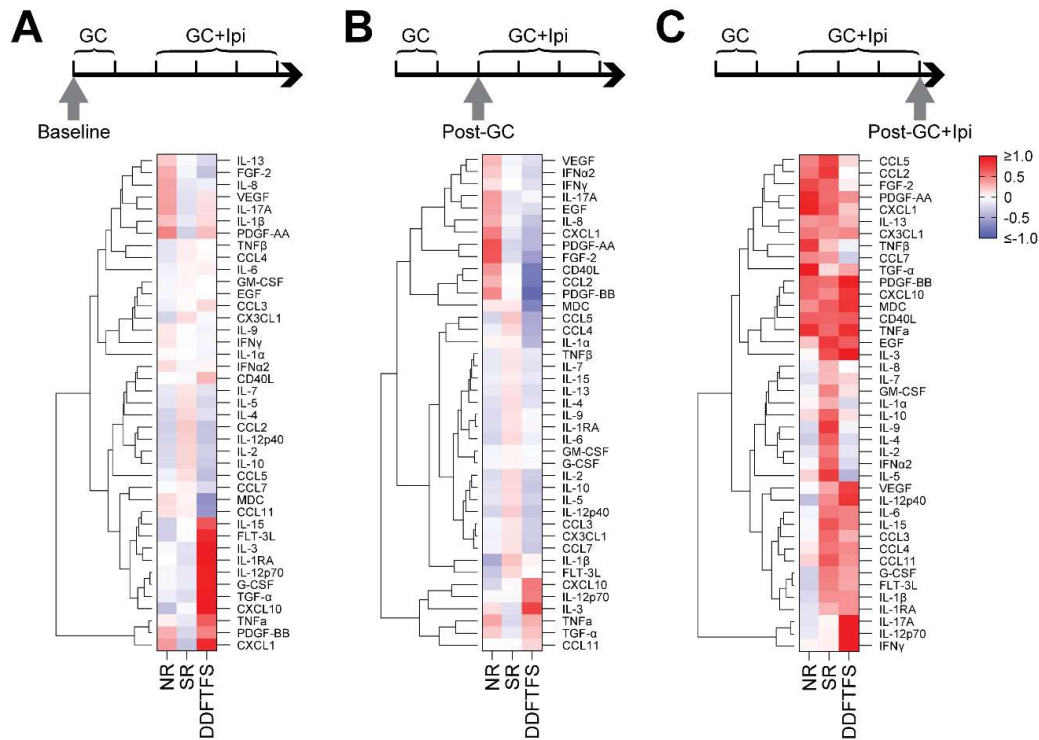
## 76 **ELISpot**

77 CD4<sup>+</sup> and CD8<sup>+</sup> T cells were isolated from PBMCs at baseline, cycle 3 day 1, and cycle 6 day 1,  
78 using magnetic beads (Invitrogen). 500,000 cells/well were plated in RPMI with 10% human AB  
79 serum (complete medium; Sigma-Aldrich) in 96-well round-bottom culture plates (Gibco).  
80 Remaining cells were pulsed with cognate pools of up to 20 polypeptides (1 µg/ml) overnight,  
81 irradiated, and co-cultured 1:1 with CD4<sup>+</sup> and CD8<sup>+</sup> T cells in complete medium supplemented  
82 with IL-2 (10 IU/ml; Roche) and IL-7 (20 IU/ml; R&D Systems). Remaining PBMCs were used to  
83 generate autologous antigen-presenting cells (APCs), which were expanded with recombinant  
84 CD40L and IL-21. After 20 (CD4<sup>+</sup>) or 10 (CD8<sup>+</sup>) days, T cells were co-cultured for 18 hours in  
85 ELISpot 96-well nitrocellulose plates (Millipore Sigma, MSHAS4510) coated with anti-IFN-γ  
86 monoclonal antibody (4 µg/ml) at 1:1 and 1:5 ratios with APCs that had been pulsed overnight  
87 with peptide subpools of 6-7 peptides or DMSO vehicle as a negative control. Stimulation with  
88 phorbol 12-myristate 13-acetate (PMA)/ionomycin served as a positive control. ELISpot  
89 processing and data extraction were performed per manufacturer instructions (CTL ImmunoSpot,  
90 Cellular Technology Limited). Reactivity was quantified as the percentage of the well stained,  
91 subtracted by that of the negative control and normalized to that of the positive control. A well was  
92 considered positive for neoantigen reactivity if spots comprised ≥5% of the well area and the  
93 stained area was ≥5-fold increased from that of the respective negative control well.

94

## 95 **REFERENCES**

- 96 1. Network TCGAR. Comprehensive Molecular Characterization of Urothelial Bladder Carcinoma.  
97 Nature. 2014;507:315.  
98



99

100 **Supplemental Figure S1**

101 DDTFS patients demonstrate unique patterns of analyte expression. Heatmaps of average z-

102 scores per response grouping at (A) baseline, (B) post-GC, and (C) post-GC+Ipi with the Milliplex

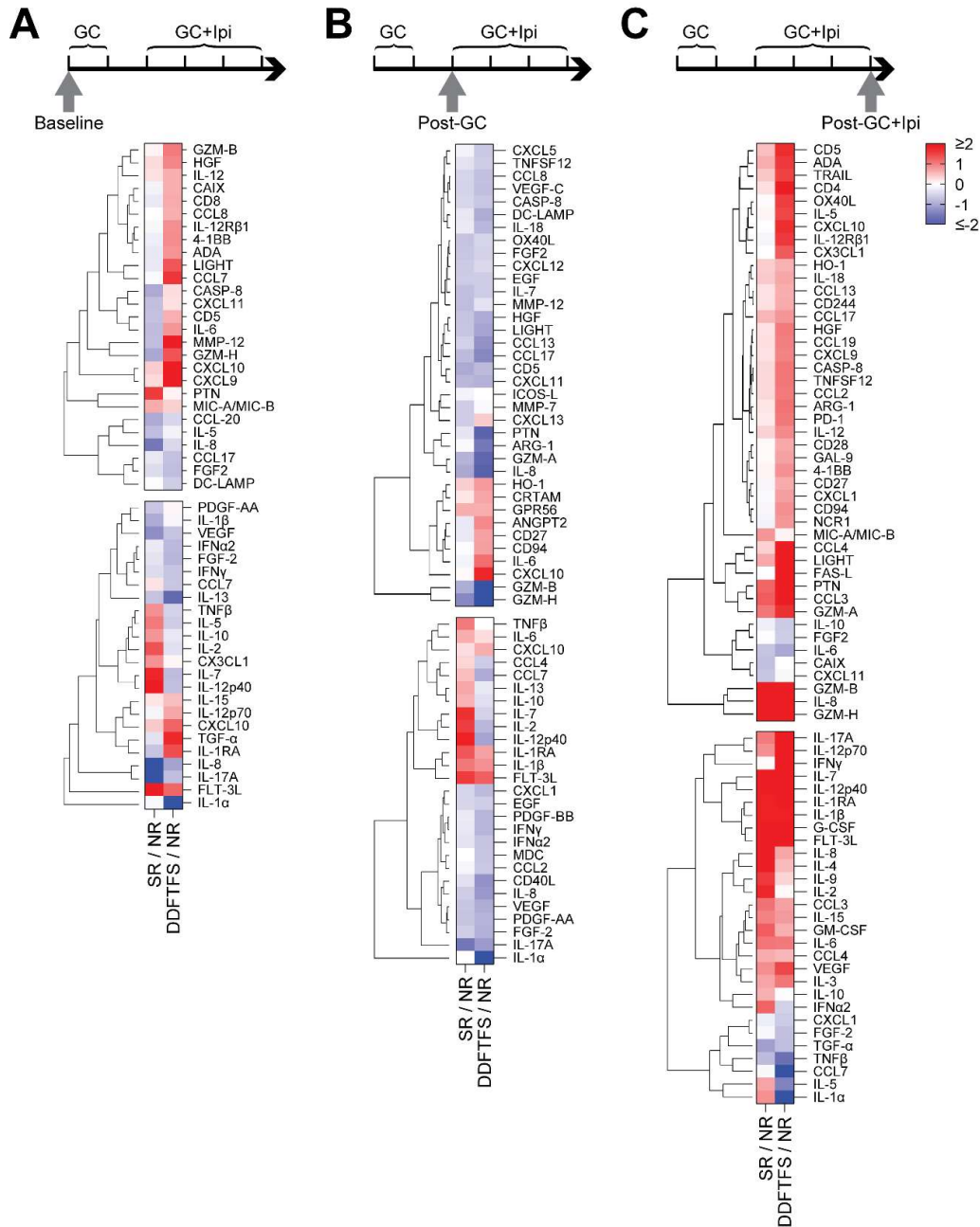
103 assay. Columns indicate patient grouping by response, rows indicate individual analytes, with

104 unsupervised hierarchical clustering performed on rows. GC, gemcitabine and cisplatin; Ipi,

105 ipilimumab; NR, non-responder; SR, short-responder; DDTFS, durable disease-free treatment-

106 free survival.

107



108

109 **Supplemental Figure S2**

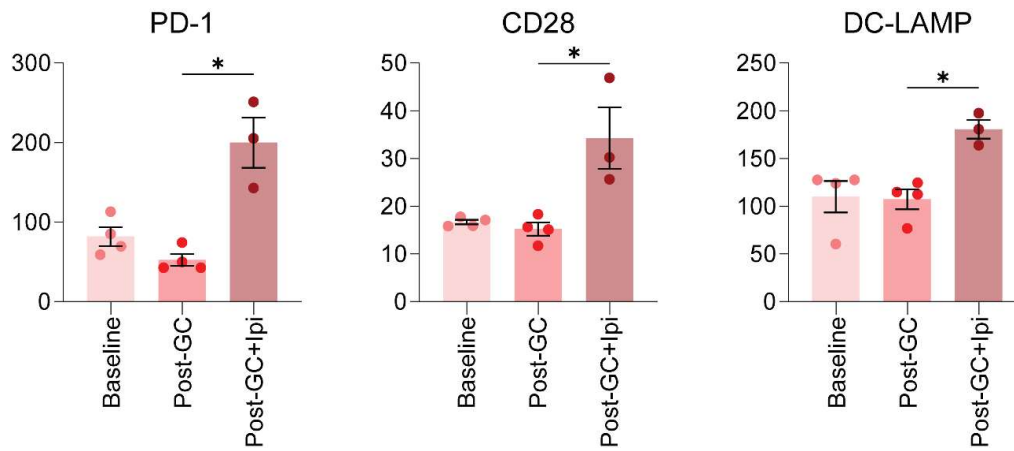
110 DDFTFs patients demonstrate a unique immunophenotype normalized to non-responders.

111 Heatmaps of all analytes with a  $\geq 1.5$ -fold increased or decreased z-score when comparing either

112 short-responders or DDFTFS patients to non-responders at (A) baseline, (B) post-GC, and (C)  
113 post-GC+Ipi. Columns indicate patient grouping normalized to NR values, rows indicating  
114 individual analytes, with unsupervised hierarchical clustering performed on rows. Olink assay on  
115 top, Milliplex assay on bottom. GC, gemcitabine and cisplatin; Ipi, ipilimumab; NR, non-responder;  
116 SR, short-responder; DDFTFS, durable disease-free treatment-free survival.

117





118

119 **Supplemental Figure S3**

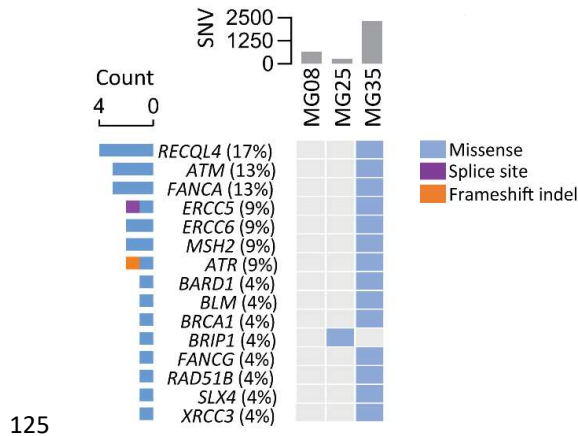
120 PD-1, CD28, and DC-LAMP increased among DDFTFS patients post-GC+Ipi. Scatter bar plots of

121 individual analytes with significantly altered levels when comparing DDFTFS patients at different

122 timepoints, with data displayed as mean  $\pm$  SEM. Y-axis is transformed NPX values. \* P < 0.05.

123 GC, gemcitabine and cisplatin; Ipi, ipilimumab.

124



125

126 **Supplemental Figure S4**

127 Heterogeneity in DDR alterations among DDFTFS patients. Percentage and type of alterations  
 128 among the entire cohort indicated on the left per gene. Total SNV count per DDFTFS patient  
 129 indicated on top. SNV, single nucleotide variant; DDR, DNA damage response; DDFTFS, durable  
 130 disease-free treatment-free survival.

131

Group		Patient ID	Best response	Time from treatment initiation to death or censor (months)	Time from treatment initiation to last follow up if alive (months)
<b>DDFTFS</b> No evidence of disease and >2 years off all treatment at time of last follow-up N=4		MG08	CR		84.2
		MG25	CR		95.0
		MG35	CR		90.9
		MG36	CR		60.3
<b>Non-DDFTFS</b> N=32	<b>Short-Responder</b> Best response CR or PR with recurrence of disease N=21	MG01	PR	6.9	
		MG02	CR	34.8	
		MG03	PR	10.6	
		MG04	PR	7.3	
		MG06	PR	26.6	
		MG10	PR	9.5	
		MG11	CR	18.4	
		MG13	CR	27.3	
		MG14	PR	10.4	
		MG17	PR	12.2	
		MG18	PR	12.3	
		MG19	PR	10.1	
		MG21	PR	2.8	
		MG22	PR	13.8	
		MG23	PR	15.0	
		MG26	PR	16.5	
		MG29	PR	23.5	
		MG30	PR	5.6	
		MG32	CR	26.9	
		MG34	PR	37.4	
		MG37	PR	37.4	
	<b>Non-Responder</b> Best response PD or SD with recurrence of disease N=11	MG05	SD	5.0	
		MG07	SD	27.7	
		MG09	SD	10.6	
		MG12	SD	6.5	
		MG15	SD	9.8	
		MG16	SD	10.6	
		MG20	SD	14.5	
		MG27	PD	4.8	
		MG28	SD	13.9	
		MG31	SD	22.5	
		MG33	SD	6.5	

132

133 **Supplemental Table S1**

134 Patient classifications by response. DDFTFS and non-DDFTFS (short-responders and non-  
135 responders) criteria and sample size listed, with best clinical response and time from treatment  
136 initiation to death/censor or last follow up if alive. DDFTFS, durable disease-free treatment-free  
137 survival; NR, non-responder; SR, short-responder; SD, stable disease; PD, progressive disease;  
138 PR, partial response; CR, complete response.

139

<b>MG02</b>		
<b>Gene</b>	<b>Variant</b>	<b>Peptide</b>
<i>TMEM185B</i>	p.D277H	KGGNHWWFGIRRHFCQFLLEIFPFL
<i>CLSTN1</i>	p.L68V	DPPLIALDKDAPVRFAESFEVTVTK
<i>PARN</i>	p.G469D	KTSDLYQLFSAFDNIQISWIDDTSA
<i>MXRA8</i>	p.S121L	ELSASAFDDGNFLLLIRAVEETDAG
<i>MCAM</i>	p.Q356H	SDVRVSPAAPERHEGSSLTLTCEAE
<i>PARP10</i>	p.A19V	HLMPRPRVAMAEVEAGVAVEVRGLP
<i>MAP1S</i>	p.A66T	DEQLKVFVSRHSTTFSSIVKQQRSL
<i>JADE2</i>	p.D475N	YRRLKLFTHLRQNLKRVRNLCYMVT
<i>CORIN</i>	p.T155M	THSQCQMLPYHAMLTPLLSVVRNME
<i>ADCY2</i>	p.S57F	PLIVFLLLIVMGFCLALLAVFFALG
<i>TAGLN</i>	p.W55S	GRPDRGRLGFQVSLKNGVILSKLVN
<i>SEPN1</i>	p.V180A	ETMTKSKDGFLGASRLALSGLRNWT
<i>KIF1C</i>	p.P408L	SVRGALPAVSSPLAPVSPSSPTTHN
<i>SFRP1</i>	p.H267Y	DCPCHQLDNLSHYFLIMGRKVKSQY
<i>PIK3C2B</i>	p.S399C	LQEALTFTCNCSCTVDLLIYQTLCY

140

141 **Supplemental Table S2**

142 Top ranked neoantigen predictions and peptide sequences synthesized for MG02.

143

<b>MG16</b>		
<b>Gene</b>	<b>Variant</b>	<b>Peptide</b>
<i>SLC12A7</i>	p.T256M	AAAMLHNMRVYGMCTLVLMALVVFV
<i>NAA35</i>	p.Y524fs	LYSMHEYYYYIYWLSL
<i>STEAP2</i>	p.P380L	LGLLSLLAVTSILSVSNALNWREFS
<i>CMTM3</i>	p.I141N	SKAAGVFGFFATNVFATDFYLIFND
<i>CARD11</i>	p.V171M	LEDEKKQMTLTRMELLTFQERYYKM
<i>MFAP5</i>	p.R158Q	LPPRRLRRSNYFQLPPCENVDLQRP
<i>DHRS4</i>	p.Q54H	DGIGFAIARRLAHDGAHVVSRRKQ
<i>MROH1</i>	p.G421S	AVVQVISAMAHHSYLEQPGGEAMIE
<i>CROCC</i>	p.R1729W	VEESEGALRDKVWGLTEALAQSSAS
<i>HN1L</i>	p.S44L	LSGQGPWAPLQRLASTRLVSGGHEA
<i>SYVN1</i>	p.L110del	DFSPRFVALFTLLFLKCFHWLAEDR
<i>LRRC48</i>	p.K69E	RIDNLWQFENLRELQLDNNIEKIE
<i>TP53</i>	p.R273C	SGNLLGRNSFEVCVCACPGRDRRTE
<i>HJURP</i>	p.V188M	RVTPLPSLASPAMPAPGYCSRISRK
<i>SOGA2</i>	p.V586M	VEEEANILGRKIMELEVENRGLKAE

144

145 **Supplemental Table S3**

146 Top ranked neoantigen predictions and peptide sequences synthesized for MG16.

147

<b>MG18</b>		
<b>Gene</b>	<b>Variant</b>	<b>Peptide</b>
<i>MIB2</i>	p.V131fs	VQVGMRVGARRGLEVGPAGRRRGR
<i>MIB2</i>	p.V131fs	DTRPHSGRAVGPQHAHQLPRRLPGR
<i>MIB2</i>	p.V131fs	RLPGRARPAAVRQRPDRRPAPQHHL
<i>SMYD5</i>	p.L60F	IFVERPLVAAQFFWNALYRYRACDH
<i>ARL3</i>	p.T147fs	EIAEGLNLHPRPSLADPVLLSSHRR
<i>HDAC1</i>	p.H39Y	GHPMKPHRIRMTYNLLLNGLYRKM
<i>IRX5</i>	p.R269fs	RARCLRVPAGPRLSIRRLRRLLRC
<i>G2E3</i>	p.E141fs	RSYHFPCGLQRMYPVYWQFCVILL
<i>CYP4F11</i>	p.D43N	LARVLAWTYTFYNNCRRLQCFQPP
<i>SNX3</i>	p.E75Q	KESTVRRRYSDFQWLRSELERESKV
<i>GTF2IRD1</i>	p.S114L	EGRVRRVLTVALRALCPTGGPPWK
<i>ZFP36L2</i>	p.P207L	ELCRTFHTIGFCLYGPRCHFHNAD
<i>STAP2</i>	p.G173R	EAQLLLERYPECRNLRLRPSGDGAD
<i>VPS16</i>	p.E642Q	GSFHIRASYAAEQRIEGRVAALQTA
<i>ATP5SL</i>	p.E59K	ILQFLTNYFYDVKALRDYLLQREMY
<i>GP6</i>	p.S184Y	AAHSGTYRCYSFYSRDPYLWSAPSD
<i>CLMN</i>	p.P735S	PHDLFYFPHYEVSLAAVLEAYVEDP
<i>TBC1D20</i>	p.D357H	FRGLLRPEDRTKHVLTKPRTNRFVK
<i>KDM6A</i>	p.E168K	VLYVDPSFCRAKKIHLRLGLMFKVN
<i>TRA2A</i>	p.R269I	RRRSPSPYYSRYISRSRSRSPRR
<i>CCR4</i>	p.L146F	DRYLAIHVAVFSFRARTLTYGVITS
<i>ARID4A</i>	p.E1066fs	ASGTCSIIVQERRVRRGQVMEIVD
<i>ARL3</i>	p.T147fs	KSRRMEMQELREPNSVLKNTNLLLS

148

149 **Supplemental Table S4**

150 Top ranked neoantigen predictions and peptide sequences synthesized for MG18.

151

<b>MG25</b>		
<b>Gene</b>	<b>Variant</b>	<b>Peptide</b>
<i>OTOP1</i>	p.L77del	IVFVAGLLLLLAWAVHAAGV
<i>OTOR</i>	p.C37Y	ASKKLCADDEYVYTISLASAQ
<i>MTHFR</i>	p.E594K	TNAPKLQPNAVTVGI
<i>TLL1</i>	p.E496Q	CVWKITVSQSYHVGLTFQ
<i>RIC8A</i>	p.T514K	GMSPRGHLKSLQDAMCETM
<i>ITGB5</i>	p.R662T	CHSLCTDEVITWVDT
<i>KDR</i>	p.T139I	VSDQHGVVYIIENKNKTVVI
<i>MYO1C</i>	p.T1002M	VVLQSDHVIEMLTKTALSA
<i>TGFB111</i>	p.S359W	GPILDNYIWALSALWHP
<i>TP53-1</i>	p.N268fs	NLLGRTALRCVFVPVL
<i>TP53-2</i>	p.N268fs	TGAQRKRISARKGSLTTSCPQGAL
<i>TP53-3</i>	p.N268fs	ALSEHCPTTPAPLPSQRRNHWMENI
<i>TP53-4</i>	p.N268fs	RNHWMENISPFERSVGVASARC
<i>TP53-5</i>	p.PDDIEQW46del	SQAMDDLMLSFTEDPG
<i>TMEM66</i>	p.P60S	YTTSRRLDSIPQLKCV
<i>ASPM</i>	p.F2233L	YWAMKERNIQLQRYNKLHRSV
<i>PCOLCE2</i>	p.N244S	IVSERSELLIQFL
<i>NMUR2</i>	p.R153C	YVAILHPFCAKLQSTRRA
<i>SNX14</i>	p.K328R	FAEPRNRKPSVLKLEL
<i>DAPK1</i>	p.T78S	KEIQHPNVISLHEVYENKT
<i>RPS4Y1</i>	p.R148H	LVTHDARTIHYPDPVIKV
<i>CAD</i>	p.D1469H	KLVRPLGLIHVHVHL
<i>MYO3A</i>	p.Q366P	LEKCYSRDPIYVYVG
<i>SETD3</i>	p.S458F	KSVLKNHDLFVRAKMAIKL

152

153 **Supplemental Table S5**

154 Top ranked neoantigen predictions and peptide sequences synthesized for MG25.

155



<b>MG31</b>		
<b>Gene</b>	<b>Variant</b>	<b>Peptide</b>
<i>DNAJC3</i>	p.S13L	MVAPGSVTSRLGLVFPFLLVLVDLQ
<i>MSMO1</i>	p.A187T	EFQAPFGMEAETHPLETLILGTGF
<i>ACSL3</i>	p.E657K	WEELCNSCEMENKVLKVLSEAAISA
<i>PLTP</i>	p.S139L	YWFFYDGGYINALAEGVSIRTGLEL
<i>PIGU</i>	p.L207F	YPLTLFVPGLLYFLQRQYIPVKMKS
<i>ABTB1</i>	p.Q374H	PGLKRLCGRSLAHMLDEDTVVGVWR
<i>LTN1</i>	p.K279N	FYRVVTCSSLALNRLCLLPDNELD
<i>LETM1</i>	p.D174N	KHYHGFRLWINTKIAARMLWRIL
<i>ENKD1</i>	p.Q293H	ENQRLETCLKLLHSQSQLLRELVLL
<i>NAP1L2</i>	p.D435E	EVNDAIYDKIYENWMAAIEEVKAC
<i>PEX11G</i>	p.R48C	VEQCPARSEVGTCLLVVSTQLSHCR
<i>ZZEF1</i>	p.S1899F	RQRLIQPYIHNYFWLLFAALALYSA
<i>MPHOSPH9</i>	p.P476L	LPNALDDRISFSLDSVLEPSMSSPS
<i>PVR</i>	p.P129L	DEGNYTCLFVTFLQGSRSVDIWLRV
<i>WNT6</i>	p.P59L	LAGRQAELCQAELEVVAELARGARL

156

157 **Supplemental Table S6**

158 Top ranked neoantigen predictions and peptide sequences synthesized for MG31.

159

<b>MG32</b>		
<b>Gene</b>	<b>Variant</b>	<b>Peptide</b>
<i>CNOT1</i>	p.H1506P	LSVIIFFFVYIWPWALPLILNNHHI
<i>DCAF7</i>	p.D243N	KQDPNYLATMAMNGMEVVILDVRVP
<i>TAPT1</i>	p.L407F	SDSVARRMGFIPFPLAVLLIRVVTS
<i>LONP1</i>	p.S692L	ALCGLDESKAKLLSDVLTLLIKQYC
<i>RP11-766F14.2</i>	p.Q1575L	PPLPFTLQGAQPLVLCFSPSPMPAP
<i>TMEM52B</i>	p.H143Y	SLDTLPGYEEALYMSRFTVAMCGQK
<i>LINGO1</i>	p.N390fs	SRARSSRTSLMCYCPTTSPAAAPAS
<i>LINGO1</i>	p.N390fs	PESTWSQPRAMGGSQSSLMARWRC A
<i>EPN3</i>	p.P293L	EKEVRSWQGDGSLMANGAGAVVHH Q
<i>POLQ</i>	p.S679L	YRFFCLWEKLPPTLMKRVAELVGVEE
<i>KCNK1</i>	p.S9L	MLQSLAGSLCVRLVERHRSAW
<i>ADCY3</i>	p.D1018N	ERERWQHLADLANFALAMKDTLTNI
<i>GPR176</i>	p.T189M	VFAVTNVADIYAMSTCTEVWSNSLG
<i>FREM2</i>	p.M327I	NTAPKPSFVAMMIMEVDQFVLTALT
<i>HIATL2</i>	p.V117I	DVWGRKPFLLGTIFFTCFPIPLMRI
<i>IPO5</i>	p.P554A	EKFVPPYYDLFMSLKHIVENAVQK
<i>EHBP1L1</i>	p.R1380W	QALEQEQRQIDGWAAEVEMQLRSLM
<i>TNPO3</i>	p.958HSCTVPVTQECLF (stop-loss)	CWALRDFTRLFRHSCTVPVTQECLF
<i>TCTN1</i>	p.S345L	YTDAGEVTKADLLFVLGTVSSVVVP
<i>TLX1</i>	p.S228L	LEKRFHRQKYLALAERAALAKALKM
<i>PNPLA5</i>	p.T218A	ELNVFNFSFQISAENFFLGLICLIP

160

161 **Supplemental Table S7**

162 Top ranked neoantigen predictions and peptide sequences synthesized for MG32.

163

<b>MG35</b>		
<b>Gene</b>	<b>Variant</b>	<b>Peptide</b>
<i>APOBEC1</i>	p.S97F	TWFLSWSPCWECFQAIREFLSRHP
<i>ZFH3</i>	p.E209K	TFHIASSFGKWFKGPDQAFPN
<i>SCN3A</i>	p.E71K	KNLPFIYGDIPPKMVSEPLEDLDP
<i>ART1</i>	p.G180D	PRCHQVFRDVGHLRFRPA
<i>FA2H</i>	p.G30W	RRLAAGACWVRRWARLYDLSSFVRH
<i>PAK7</i>	p.D517N	VDMYSSYLVGNELWVMEFLEG
<i>TNN</i>	p.S479F	QAVIDKYVRYTFADGDTKEMAVHK
<i>AGPAT5</i>	p.F65L	RLYCVYQSMVLFLENYTGQVILLY
<i>MMP9</i>	p.F581L	SVFEERLSKKLFLFSGRQVWVYTG
<i>SLC6A6</i>	p.P253T	TGKVVYFTATFTFAMLLVLLVRGL
<i>ATP8B1</i>	p.S925Y	EGMQAVMSSDYFAQFRYLQRLLL
<i>PIEZO1</i>	p.S217L	VTLLALAGIAHPLALSSVYLLFLA
<i>FAM120C</i>	p.S583F	EASLGDGEPHIPFLLSMSTRNHMDI
<i>PAK2</i>	p.D317H	VNFLDSYLVGHELFVMEYLAGG
<i>VWF</i>	p.A1098fs	CSCESIGDCVLLRHHCCCLCPRVCPA
<i>USP24</i>	p.S2411L	LEVMFALRELTGLLLALIEVV
<i>TRAM1</i>	p.M165I	WRAYPHNLMTFQIKFFYISQLAY
<i>KIAA0922</i>	p.Q385E	KACLFSSVAEGYFRMDSSATQ
<i>PICALM</i>	p.Q521E	KPTVASENQNLPAKLP
<i>DHX9</i>	p.E358Q	GPLAFATPQQISMDLKNELMY
<i>MACF1</i>	p.S3200F	KTKETKHQIFSSNECKEKSYQE
<i>MSN</i>	p.Q48R	TIGLREVWFFGLRYQDTKGFSTWLK
<i>HDAC9</i>	p.K1002N	NMNAVISLQNIIEIQSKYWKS
<i>ZMYM6</i>	p.S282L	IPPYALGKSLRPLAEMIET
<i>HES1</i>	p.F238L	GQFAFLIPNGALAHSGPVIPIVYTS

164

165 **Supplemental Table S8**

166 Top ranked neoantigen predictions and peptide sequences synthesized for MG35.

167

Characteristic	DDFTFS (N=4)	Non-DDFTFS (N=32)
Age, median (range)	66.5 (64-72)	62 (36-82)
Sex, N (%)		
Male	4 (100)	32 (78.1)
Female	0 (0)	4 (21.9)
Baseline neutrophil-lymphocyte ratio, median (range)	4.5 (2.2-7.3)	3.0 (1.3-7.0)
Mutation count, median (range)	664 (268-2324)	639 (273-2102)
Primary Tumor, N (%)		
Bladder	3 (75)	25 (78.1)
Renal Pelvis	0 (0)	7 (21.9)
Ureter	1 (25)	0 (0)
Karnofsky performance status, N (%)		
100%	2 (50)	7 (21.9)
90%	2 (50)	12 (43.8)
80%	0 (0)	11 (34.4)
ECOG performance-status score, N (%)		
0	2 (50)	7 (21.9)
1	2 (50)	25 (78.1)
Site of metastatic disease, N (%)		
Lymph node/soft tissue only	3 (75)	17 (53.1)
Visceral	1 (25)	13 (40.6)
Liver	1 (25)	6 (18.8)
Lung	1 (25)	9 (28.1)
Bone	0 (0)	10 (31.3)
Prior treatment, N (%)		
Systemic chemotherapy	0 (0)	5 (15.6)
Cystectomy or nephroureterectomy	3 (75)	9 (28.1)
Radiation therapy	0 (0)	2 (6.25)

168

169 **Supplemental Table S9**

170 Demographic and clinical characteristics of DDFTFS and non-DDFTFS patients. DDFTFS,

171 durable disease-free treatment-free survival; ECOG, Eastern Cooperative Oncology Group.

172